1-1-2017

Lung cancer diagnosis with quantitative DIC microscopy and support vector machine

Longfei Zheng

Shuangshuang Cai

Bixin Zeng

Min Xu
Fairfield University, mxu@fairfield.edu

Peer Reviewed

Published Citation

Longfei Zheng, Shuangshuang Cai, Bixin Zeng, Min Xu, "Lung cancer diagnosis with quantitative DIC microscopy and support vector machine", Proc. SPIE 10245, International Conference on Innovative Optical Health Science, 102450K (5 January 2017); doi: 10.1117/12.2268806; https://doi.org/10.1117/12.2268806

Lung cancer diagnosis with quantitative DIC microscopy and support vector machine

Longfei Zheng, Shuangshuang Cai, Bixin Zeng, Min Xu

Longfei Zheng, Shuangshuang Cai, Bixin Zeng, Min Xu, "Lung cancer diagnosis with quantitative DIC microscopy and support vector machine," Proc. SPIE 10245, International Conference on Innovative Optical Health Science, 102450K (5 January 2017); doi: 10.1117/12.2268806

SPIE.

Event: International Conference on Innovative Optical Health Science, 2016, Shanghai Everbright International Hotel, China

Lung Cancer Diagnosis with Quantitative DIC Microscopy and Support Vector Machine

Longfei Zheng[a,b], Shuangshuang Cai[a,b], Bixin Zeng[a,b], Min Xu*[c]

[a] Department of Biomedical Engineering, Wenzhou Medical University, Wenzhou, Zhejiang, China 325035;

[b] Institute of Lasers and Biomedical Photonics, Wenzhou Medical University, Wenzhou, Zhejiang, China 325035;

[c] Department of Physics, Fairfield University, 1073 North Benson Road, Fairfield, CT USA 06824

ABSTRACT

We report the study of lung squamous cell carcinoma diagnosis using the TI-DIC microscopy and the scattering-phase theorem. The spatially resolved optical properties of tissue are computed from the 2D phase map via the scattering-phase theorem. The scattering coefficient, the reduced scattering coefficient, and the anisotropy factor are all found to increase with the grade of lung cancer. The retrieved optical parameters are shown to distinguish cancer cases from the normal cases with high accuracy. This label-free microscopic approach applicable to fresh tissues may be promising for in situ rapid cancer diagnosis.

Keywords: TI-DIC; Scattering-Phase theorem; Scattering Coefficient; Reduced Scattering Coefficient; Anisotropy Factor; Support Vector Machine; Squamous Cell Lung Cancer

1. INTRODUCTION

Pathological examination is currently the gold standard for cancer diagnosis. Traditional pathological diagnosis requires tissue preparation, which includes multiple time consuming steps, and is not suitable for in situ diagnosis. It also suffers from the inter- and intra-observer variance due to its subjective nature. In last two decades, much efforts have been devoted to developing new label-free optical techniques for in situ rapid cancer diagnosis.

Light scattering by cells or tissues has important applications in disease diagnosis as the wavelength of light in the visible and near-infrared wavebands is close to the characteristic scale of the structures in cells and tissue[1]. Light scattering can reveal the changes in the morphology, composition and physiological state and has been successfully used in detecting the sub-wavelength scale morphological and biochemical changes in tissues[2-4].

Phase imaging has been widely used to probe the microstructure changes in transparent specimens. Compared to other phase-imaging techniques, the differential interference contrast (DIC) microscope is popular owing to its higher transverse resolution, better depth discrimination, and the pseudo-3D relief type of image that is clear of artifacts. However, the resulting image of commercial DIC microscope cannot be used directly for quantitative analysis, as the image intensity is not linearly proportional to the phase information. Kou et al. found that by taking a through-focus series of images and with the transport-of-intensity equation (TIE), quantitative phase image can be retrieved from DIC microscope images[5,9]. The method named as TI-DIC is robust and requires no or minimal hardware modifications.

In this paper, we performed a study on lung cancer diagnosis using the TI-DIC method together with the scattering-phase theorem we reported before[6,7]. Two-dimensional quantitative phase maps of pathological sections for 80 normal lung

International Conference on Innovative Optical Health Science, edited by Xingde Li, Qingming Luo, Proc. of SPIE Vol. 10245, 102450K · © 2017 SPIE · CCC code: 1605-7422/17/$18 · doi: 10.1117/12.2268806

cases and 180 squamous cell lung cancer cases were obtained first using TI-DIC. The scattering coefficient (μ_s), the reduced scattering coefficient (μ_s'), and the anisotropy factor (g) of each case were then computed based on the scattering-phase theorem. A strong correlation between the light scattering parameters of tissue and the grade of lung cancer is observed. When lung cancer progresses, the scattering coefficient, the reduced scattering coefficient, and the anisotropy factor all increase. An accuracy of 98.9% has been achieved in distinguishing cancer cases from normal cases using a support vector machine (SVM) classifier based on the recovered light scattering parameters of tissue alone.

2. THEORY

As the consequence of free-space Helmholtz wave equation, TIE under the paraxial approximation outlines an elliptical second-order partial differential equation that recovers phase from a through-focus series of image intensities. Consider a complex plane wave travailing along the z direction:

$$E(x,y,z)=\sqrt{I(x,y,z)}e^{i[kz+\varphi(x,y,z)]} \tag{1}$$

The phase immediately after the object can be retrieved through[8]:

$$\nabla_{\perp}[I(x,y,z)\nabla_{\perp}\varphi(x,y,z)]=-k\frac{\partial I}{\partial z} \tag{2}$$

where k is the wave number, the terms I (x, y, z), φ(x, y, z), and $\frac{\partial I}{\partial z}$ denote the in-focus image intensity, phase to be retrieved, and longitudinal derivative of the intensity, respectively. The 2D gradient operator $\nabla_{\perp}$ operates on the transverse direction alone. By applying Fourier transform, the phase on the in-focus plane is obtained as following[8]:

$$\varphi(r_{\perp},z)=\mathrm{F}^{-1}\mathrm{q}_{\perp}^{-2}\mathrm{F}\left[k\frac{\partial \ln I}{\partial z}\right] \tag{3}$$

where $q_{\perp}$, F and F^{-1} are the transverse spatial frequency, symbols representing Fourier transform and inverse Fourier transform, respectively, and $r_{\perp}$ is the 2D position in the transverse plane normal to the optical axis z. The term $\frac{\partial \ln I}{\partial z}$ can be approximated by:

$$\frac{\ln I(x,y,\Delta z)-\ln I(x,y,0)}{\Delta z} \tag{4}$$

and

$$\frac{\ln I(x,y,0)-\ln I(x,y,-\Delta z)}{\Delta z} \tag{5}$$

where I(x, y, 0), I(x, y, Δz) , I(x, y, -Δz) are light intensity at the in-focus plane and planes below or above at a distance of Δz away.

The scattering-phase theorem is then applied to determine μ_s, μ_s' and g from the measured phase map. The relationship between μ_s, μ_s' , g and the 2-D phase map (φ) has been derived earlier and is given by the following formulas[6]:

$$\mu_S L=2\langle 1-\cos\Delta\varphi\rangle \tag{6}$$

$$\mu_S' L = \frac{1}{2k^2}\langle|\nabla\varphi|^2\rangle \tag{7}$$

$$g = 1 - \frac{\langle|\nabla\varphi|^2\rangle}{4k^2\langle 1-\cos\Delta\varphi\rangle} = 1 - \frac{\mu_s'}{\mu_s} \tag{8}$$

where L is the thickness of the thin specimen, $\langle\ \rangle$ means the spatial average, $\Delta\varphi = \varphi - \langle\varphi\rangle$, and

$$|\nabla\varphi|^2 = \left(\frac{\partial\varphi}{\partial x}\right)^2 + \left(\frac{\partial\varphi}{\partial y}\right)^2.$$

3. EXPERIMENTS AND RESULTS

The system was built on a commercial DIC microscopy (Observer A1, Zeiss). The light source was a Halogen 100W lamp filtered by a 550nm narrow-band filter under Köhler illumination. The numerical aperture for the condenser and objective (Plan-Neofluar 40×) were 0.3 and 0.75， respectively. The pixel size for the recorded images was 0.082μm using a CCD camera from Zeiss (AxioCam ICC5). A three-dimensional scanning stage with a z-encoder (Pro Scan III, Prior) was used to take in-focus and out-of-focus images (Δz=1μm) automatically.

To validate the performance and stability of the system, we first measured the light scattering properties of polystyrene spheres and compared the results with the theoretical prediction obtained by Mie theory. The polystyrene spheres (10μm in diameter) suspension was diluted with water and deposited on a glass microscope slide and covered with a slide cover. Three images, one in-focus and two out-of-focus, were taken for the monolayer of polystyrene sphere suspension. The out-of-focus images were taken on planes with 1μm distance below and above the in-focus plane. The quantitative phase map of the polystyrene sphere suspension was retrieved by the TI-DIC algorithm. The scattering properties for each individual sphere were analyzed by applying the scattering-phase theorem to the region in the phase map being occupied by the sphere. Results of the retrieved phase map, the gradient of phase map, and the scattering properties of the sphere were shown in figure 1. The average of scattering coefficient, reduced scattering coefficient and anisotropy factor obtained were μ_s = 0.208172 μm^{-1}, μ_s' = 0.018177μm^{-1}, and g = 0.912683 respectively. The results were in good agreement with theoretical prediction (μ_s = 0.22986 μm^{-1}, μ_s' = 0.021003μm^{-1}, and g = 0.908628) computed with a Mie code.

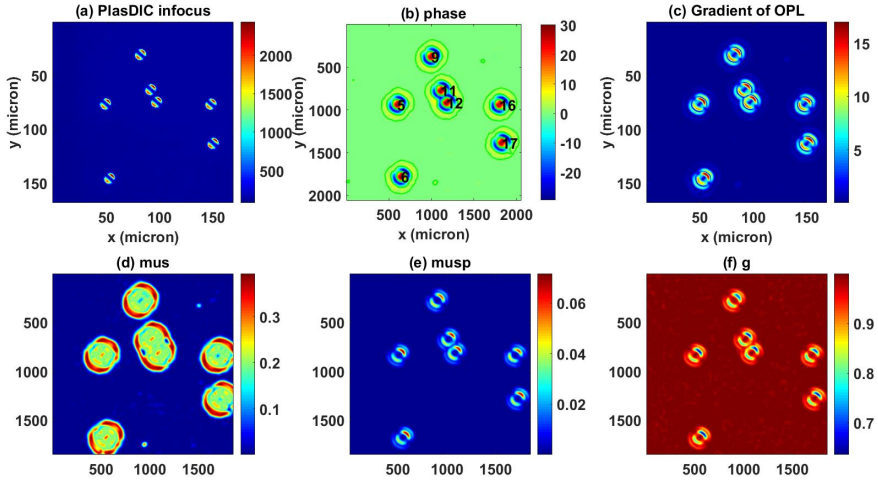

Figure 1 Imaging 10μm polystyrene spheres. (a) The original image obtained on the focus plane; (b) the retrieved 2-D phase map; (c) the gradient of phase map; (d) the scattering coefficient (μm^{-1}); (e) the reduced scattering coefficient (μm^{-1}); and (f) the anisotropy factor.

Tissue microarrays of squamous cell lung cancer and normal lung tissue were then used in the following study. The tissue microarrays (one stained and two unstained slides) were bought from Biomax Inc. which includes pathology diagnosis information of grades, stages, and TNM grading. First, we identified the characteristic location for each case using the H&E stained slide in bright-field microscopy. The DIC images of in-focus and out-of-focus of the un-stained slides were then taken at the corresponding location for each ease. The 2-D phase maps and the scattering properties were computed afterwards. The μ_s, μ_s' and g of squamous cell lung cancer with different grades were illustrated in figure 2 and figure 3. It was found the scattering coefficient, the reduced scattering coefficient, and the anisotropy factor all increase for cancer cases with higher tumor grade. Table 1 summarizes the scattering parameters of normal and cancerous lung tissue of different grades.

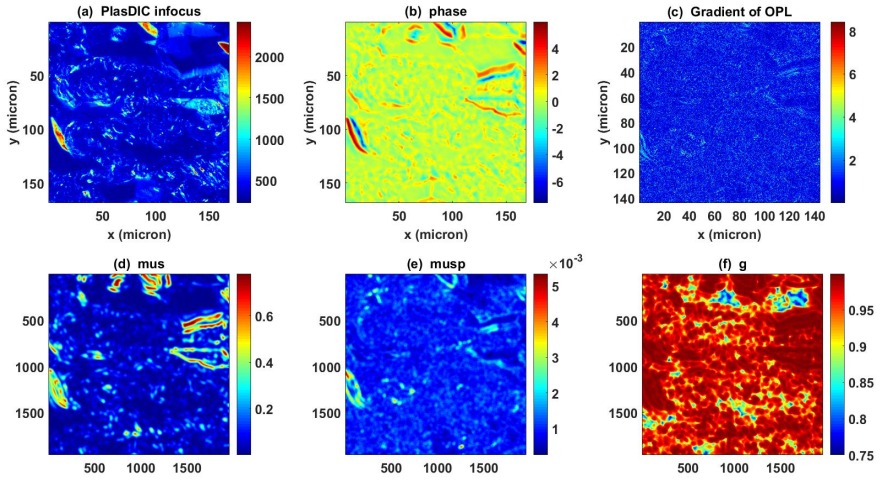

Figure 2 Imaging low grade cancer. (a) The original image obtained on the focus plane; (b) the retrieved 2-D phase map; (c) the gradient of phase map; (d) the scattering coefficient (μm^{-1}); (e) the reduced scattering coefficient (μm^{-1}); and (f) the anisotropy factor.

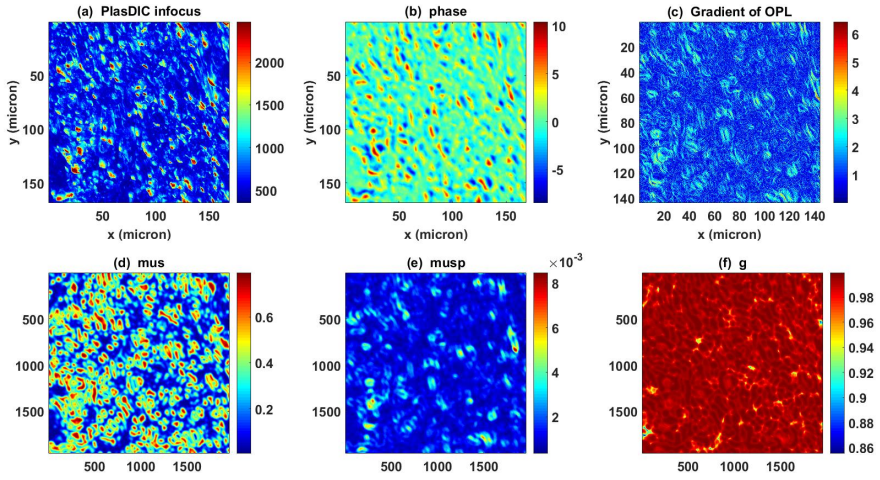

Figure 3 Imaging high grade cancer. (a) The original image obtained on the focus plane; (b) the retrieved 2-D phase map; (c) the gradient of phase map; (d) the scattering coefficient (μm^{-1}); (e) the reduced scattering coefficient (μm^{-1}); and (f) the anisotropy factor.

Scattering Parameter	Normal	Grade 1	Grade 2	Grade 3
μ_s (μm^{-1})	0.116 (0.047)	0.165 (0.041)	0.203 (0.042)	0.250 (0.050)
μ_s' (μm^{-1})	0.0004 (0.0001)	0.015 (0.004)	0.022 (0.009)	0.028 (0.012)
g	0.996 (0.0006)	0.968 (0.025)	0.981 (0.016)	0.988 (0.013)

Table 1 The scattering parameters of normal and cancerous lung tissue of different grades. The number in parenthesis represents the standard deviation among the group of specimens.

4. TRAINING AND PREDICTING

A support vector machine (SVM) classifier was trained to perform diagnosis using the scattering parameters obtained above. All the cases (normal and cancer) were divided into two groups, one for training and the other for prediction. For normal cases, the number of cases for training and prediction are 60 and 20, respectively. For cancer cases, the number of cases for training and prediction are 100 and 80, respectively. The function mapminmax (Matlab) was used to normalize the scattering parameters; the function svmtrain was used to obtain the classification model; and the function svmpredict was used to perform prediction. A receiver operating characteristic curve (ROC) was utilized to assess the performance of classification. The ROC curve was plotted based on the true positive rate (TPR) vs the false positive rate (FPR) at various threshold. Through optimizing the SVM penalty parameter and kernel parameter, a predicting accuracy of 98.9% was achieved (see figure 4).

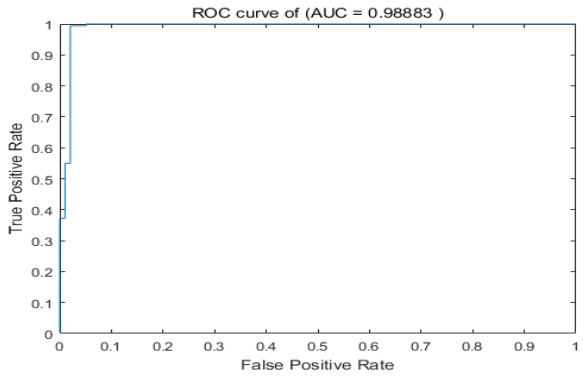

Figure 4 ROC curve for distinguishing normal and cancerous lung tissue.

5. DISCUSSION AND CONCLUSION

The preliminary results show that scattering properties differ significantly between normal and cancerous lung tissue of various grades. This is related to the microstructure alterations when cancer progresses. The scattering coefficient (μ_s) and the reduced scattering coefficient (μ_s') reflect the total and weighted scattering power of tissue. Both μ_s and μ_s' are observed to increase steadily from normal to cancer and with the cancer grade. This suggests an overall fragmentation of structures in tissue with cancer progression. TI-DIC microscopy together with the scattering-phase theorem is effective in quantifying the microstructural alterations in tissue.

In summary, we have demonstrated a microscopic approach to map the light scattering parameters of tissue based on the TI-DIC method and the scattering-phase theorem. A strong correlation between light scattering parameters of tissue and the grade of lung cancer has been observed. Optical parameters has been shown to distinguish cancer cases from normal cases with high accuracy. As the proposed method is label-free and can be applied to fresh tissues, it may emerge as a promising in situ rapid optical pathology for cancer diagnosis.

ACKNOWLEDGMENTS

This work is supported by National Natural Science Foundation of China (81470081), Key Project of Natural Science Fo undation of Zhejiang Provinces (LZ16H180002), and Fundamental Research Funds of Wenzhou Medical University (89 213018).

REFERENCES

[1] Xu, M., and R. R. Alfano, "Fractal mechanisms of light scattering in biological tissue and cells," Optics Letters 30(22), 3051-3 (2005).
[2] Müller, Markus G., et al, "Spectroscopic detection and evaluation of morphologic and biochemical changes in early human oral carcinoma †," Cancer 97(7), 1681-92 (2003).
[3] Wang, Z., et al, "Tissue refractive index as marker of disease," Journal of Biomedical Optics 16(11), 631-648 (2011).
[4] Uttam, S, et al, "Correction of stain variations in nuclear refractive index of clinical histology specimens," Journal of Biomedical Optics 16(11), 116013-116013-7 (2011).
[5] Shan, Shan Kou, et al, "Transport-of-intensity approach to differential interference contrast (TI-DIC) microscopy for quantitative phase imaging," Optics Letters 35(3), 447-9 (2010).
[6] Xu, Min, "Scattering-phase theorem: anomalous diffraction by forward-peaked scattering media," Optics Express 19(22), 21643-51 (2011).
[7] Mariam Iftikhar; Bianca DeAngelo; Grant Arzumanov; Patrick Shanley; Zhang Xu; and M. Xu. “Characterizing scattering property of random media from phase map of a thin slice: the scattering-phase theorem and the intensity propagation equation approach.” In Optical Tomography and Spectroscopy of Tissue IX, Proc. SPIE 7896, 78961O (2011).
[8] Allen, L. J., and M. P. Oxley, "Phase retrieval from series of images obtained by defocus variation," Optics Communications 199(1-4), 65-75 (2001).
[9] Aung, H., Buckley, J., Kostyk, P., Rodriguez, B., Phelan, S., & Xu, M. “Three dimensional refractive index imaging with differential interference contrast microscopy.” In Jose-Angel Conchello, C. J. Cogswell, T. Wilson, & T. G. Brown (Eds.), Three-Dimensional and Multidimensional Microscopy: Image Acquisition and Processing XIX. Proc. SPIE. 8227, 82270G-82270G-8 (2012).